Performance evaluation of multiple satellite rainfall products for Dhidhessa River Basin (DRB), Ethiopia

Gizachew Kabite Wedajo[a,b*], Misgana Kebede Muleta[c], Berhan Gessesse Awoke[b,d]

[a]Department of Earth Sciences, Wollega University, P.O.Box 395, Nekemte, Ethiopia

[b]Department of Remote Sensing, Entoto Observatory Research Center, Ethiopia Space Science Technology Institute, P.O.Box 33679, Addis Ababa, Ethiopia

[c]Department of Civil and Environmental Engineering, California Polytechnic State University, San Luis Obispo, California, 93407

[d]Department of Geography and Environmental Studies, Kotebe Metropolitan University, Addis Ababa, Ethiopia

*Correspondence: Email: Kabiteg@gmail.com

Abstract

Precipitation is crucial driver of hydrological processes. Ironically, a reliable characterization of its spatiotemporal variability is challenging. Ground-based rainfall measurement using rain gauges is more accurate. However, installing a dense gauging network to capture rainfall variability can be impractical. Satellite-based rainfall estimates (SREs) could be good alternatives, especially for data-scarce basins like in Ethiopia. However, SREs rainfall is plagued with uncertainties arising from many sources. The objective of this study was to evaluate the performance of the latest versions of several SREs products (i.e., CHIRPS2, IMERG6, TAMSAT3 and 3B42/3) for the Dhidhessa River Basin (DRB). Both statistical and hydrologic modelling approaches were used for the performance evaluation. The Soil and Water Analysis Tool (SWAT) was used for hydrological simulations. The results showed that whereas all four SREs products are promising to estimate and detect rainfall for the DRB, the CHIRPS2 dataset performed the best at annual, seasonal and monthly timescales. The hydrologic simulation based evaluation showed that SWAT's calibration results are sensitive to the rainfall dataset. The hydrologic response of the basin is found to be dominated by the subsurface processes, primarily by the groundwater flux. Overall, the study showed that both CHIRPS2 and IMERG6 products could be reliable rainfall data sources for hydrologic analysis of the DRB. Moreover, climatic season of the DRB influences rainfall and streamflow estimation. Such information is important for rainfall estimation algorithm developers.

Keywords: *Satellite-based rainfall estimates; Dhidhessa River Basin; Performance evaluation; Statistical evaluation; Hydrological modelling performance.*

1. Introduction

Precipitation is an important hydrological component (Behrangi et al., 2011; Meng et al., 2014). Accurate representation of its spatiotemporal variability is crucial to improves hydrological modelling (Grusson et al., 2017). Ironically, precipitation is one of the most challenging hydrometeorological data to be accurately represented (Yong et al., 2014). Climatic and topographic conditions are the primary factors that affect the accuracy of rainfall measurements.

Rainfall is measured either using ground-based (i.e., rain gauge and radar) or satellite sensors, where all measurement methods exhibit limitations (Thiemig et al., 2013). In addition, Commercial Microwave Links (CML) is introduced recently as cheap and fast rainfall estimation method (Smiatek et al., 2017) but not fully tested methodology (Nebuloni et al., 2020). Ground-based rainfall measurements using rain gauge is a direct and generally accurate near the sensor location. However, rain gauges, for instant, either are of poor density to represent spatial and temporal variability of precipitation, or may not even exist in many basins especially in developing countries (Behrangi et al., 2011). Rain gauge based rainfall measurement techniques provide point measurements and subject to missing data due to mainly measurement errors (Kidd et al., 2012; Maggioni et al., 2016). It may also be infeasible to install and maintain dense ground-based gauging stations in remote areas like mountains, deserts, forests and large water bodies (Dinku et al., 2018; Tapiador et al., 2012). On the other hand, radar-based rainfall measurement technique covers larger area and provides rainfall data at high spatial and temporal scales (Sahlaoui and Mordane, 2019). However, radar rainfall measurements have limitations due to attenuation of radar signal by several features that negatively affect the quality of rainfall measurement (Villarini and Krajewski, 2010; Berne and Krajewski, 2013; Sahlaoui and Mordane, 2019). Satellite-based rainfall estimates (SREs), however, provide high-resolution precipitation data including in areas where ground-based rainfall measurements are impractical, sparse, or non-existent (Stisen and Sandholt, 2010).

Consequently, high-resolution precipitation products have been developed over the last three decades. These products include Tropical Rainfall Measuring Mission (TRMM) Multi-satellite Precipitation Analysis (TMPA; Huffman et al., 2007), the Precipitation Estimation from Remote Sensing Information Using Artificial Neuron Networks (PERSIANN; Sorooshian et al., 2000), Climate Prediction Center (CPC) morphing algorithm (CMORPH) (Joyce et al., 2004), African Rainfall Climatology (ARC) (Xie and Arkin 1995), Tropical

Applications of Meteorology using SATellite (TAMSAT) (Maidment et al., 2017) and the Climate Hazards Group InfrareRed Precipitation with Stations (CHIRPS) (Funk et al., 2015). The consistency, spatial coverage, accuracy and spatiotemporal resolution of SREs have been improved over time (Behrangi et al., 2011).

As indirect rainfall estimation techniques, SREs products possess uncertainties resulting from errors in measurement, sampling, retrieval algorithm, and bias correction processes (Dinku et al., 2010; Gebremichael et al., 2014; Tong et al., 2014). Local topography and climatic conditions can also affect the accuracy of SREs estimation (Bitew and Gebremichael, 2011). Hence, SREs products should be carefully evaluated before using the products for any application. Statistical and hydrological modelling are two common methods for evaluating SREs. The statistical evaluation method examines the intrinsic precipitation data quality including its spatiotemporal characteristics via pairwise comparison of the SREs products and ground observations. Scale mismatches between area-averaged SRE data and point-like ground-based measurements is the most critical drawback. The hydrological modelling method evaluates the performance of a SREs product for a specific application such as streamflow predictive ability at watershed scale (Su et al., 2017). The two methods complement each other where the statistical method provides information on data quality while the hydrological model technique assesses the usefulness of the data for hydrological applications (Thiemig et al., 2013). However, most studies used only statistical evaluation methods (e.g., Dinku et al., 2018; Ayehu et al., 2018).

Studies have recommended SREs products for data scare basins (Behrangi et al., 2011; Bitew and Gebremichael, 2011; Thiemig et al., 2013). However, there is no consensus regarding "best" SREs product for different climatic regions. Nesbitt et al. (2008) found that CMORPH and PERSIANN produced higher rainfall rates compared to TRMM for the mountain ranges of Mexico. Dinku et al. (2008) reported better performance of the TRMM and CMORPH products in Ethiopia and Zimbabwe whereas PERSIANN outperformed TRMM in South America according to de Goncalves et al. (2006). Interestingly, the performance of SREs products seems to differ even within a basin. For the Blue Nile basin in Ethiopia, for example, CMORPH overestimated precipitation for the lowland areas but underestimated for the highlands (Bitew and Gebremichael, 2011; Habib et al., 2012; Gebremichael et al., 2014). The discrepancy in the findings of these studies shows the performance of SREs varies with region, topography, season, and climatic conditions of the study area (Kidd and Huffman, 2011;

99 Seyyedi et al., 2015; Nguyen et al., 2018; Dinku et al., 2018). As such, many studies have
100 recommended SREs evaluation at a local scale to verify its performance for specific
101 applications (Hu et al., 2014; Toté et al., 2015; Kimani et al., 2017; Ayehu et al., 2018).

102 Studies have examined the performance of SREs in Ethiopia (Haile et al., 2013;
103 Worqlul et al., 2014; Ayehu et al., 2018; Dinku et al., 2018). However, majority of these studies
104 used the statistical method to evaluate SREs, and no study has been completed for the
105 Dhidhessa River Basin (DRB). With only 0.32 rain gauges per 1000 km^2, the DRB meets the
106 World Meteorological Organization (WMO) data-scarce basin classification (WMO, 1994).
107 Evaluating the performance of various SREs products in terms of characterizing the
108 spatiotemporal distribution of rainfall in the DRB could assist with the planning and
109 management of existing and planned water resources projects in the river basin.

110 SREs have been continuously updated to minimize bias and uncertainty. Evaluating
111 and validating improved products for various climatic regions would be valuable (Kimani et
112 al., 2017). Recently improved SREs products include Tropical Rainfall Measuring Mission
113 (TRMM) Multi-Satellite Precipitation Analysis version 7 (here after referred to as 3B43 for
114 monthly and 3B42 for daily products), Climate Hazards Group InfrareRed Precipitation with
115 Stations version 2 (CHIRPS2), Tropical Applications of Meteorology using SATellite version
116 3 (TAMSAT3) and Integrated Multi-satellitE Retrievals for GPM version 6B (IMERG6).
117 Studies have reported improvements of these new versions compared to their predecessors.
118 However, to the best of authors' knowledge, the rainfall detection and hydrological simulation
119 capability of these SREs datasets were not evaluated for the basins in Ethiopian including the
120 DRB. This study examined the latest SREs products in terms of their rainfall detection and
121 estimation skills, and improving hydrological prediction for DRB, a medium-sized river basin
122 with scarce gauging data. As such, the objectives of this study were: 1) to evaluate the intrinsic
123 rainfall data quality and detection skills of multiple SREs products (i.e., 3B42/3, CHIRPS2,
124 TAMSAT3, and IMERG6), and 2) to examine hydrologic prediction performances of SREs for
125 the DRB. The Soil and Water Assessment Tool (SWAT), a physically based semi-distributed
126 model that has performed well in humid tropical regions like Ethiopia, was used for the
127 hydrologic simulation.

128

2. Methods and Materials

2.1. Descriptions of the study area

The Dhidhessa River drains to the Blue Nile River (Figure 1). It is one of the largest and most important river basins in Ethiopia in terms of its physiography and hydrology (Yohannes, 2008). Located between 7˚42'43"N to 10˚2'55"N latitude and 35˚31'23"E to 37˚7'60"E longitude, the river basin exhibits highly variable topography that ranges from 619 m to 3213 m above mean sea level (a.m.s.l). The Dhidhessa River starts from the Sigmo mountain ranges and travels 494 km before it joins the Blue Nile River around the Wanbara and Yaso districts. The outlet considered for this study is the confluence of the Dhidhessa River and the Blue Nile River which covers a total drainage area of 28,175 km^2. The River basin has many perennial tributaries (Figure 1).

Temperature and precipitation in the Dhidhessa River basin exhibit substantial spatial and seasonal variability. The mean maximum and minimum daily air temperatures in the river basin range from 20-33˚C and 6-19 ˚C, respectively. The long-term mean annual rainfall ranges from 1200 mm to 2200 mm in the river basin. Soils in the DRB are generally deep and have high organic content implying they have high infiltration potential. The dominant soil type is Acrisols while Cambisols and Nitisols are common (OWWDSE, 2014). Igneous, sedimentary and metamorphic rocks are common but igneous rock, particularly basalt, is dominant in the basin (GSE, 2000). Forest, shrubland, grassland, and agriculture are the dominant land cover types in the basin (Kabite et al., 2020). Major crops include perennial and cash crops like coffee, Mango, and Avocado (OWWDSE, 2014).

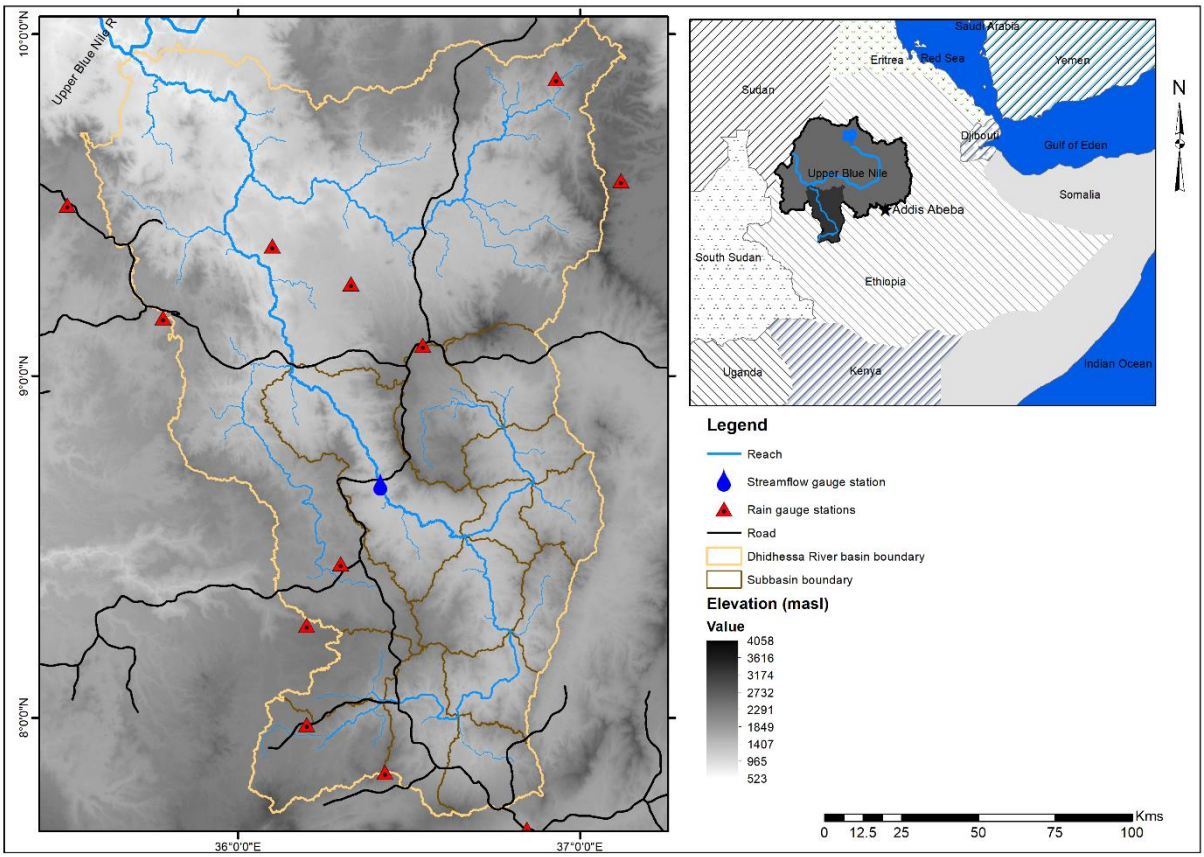

Figure 1. Location map of Dhidhessa River basin with ground stations (USGS, 1998).

2.2. Data sources and descriptions

For this study, we used different spatial and temporal datasets such as Digital Elevation Model (DEM), climate, streamflow, soil and land cover from different sources (Table 1).

Table 1. Data description and sources.

Data type	Data periods	Resolution	Sources
SRTM DEM	1998	30 * 30 m	USGS
3B42/3	2001-2014	0.25°(~25 km)	NASA & JAXA
CHIRPS2	2001-2014	0.05° (~5 km)	USGS & Climate Hazard Group
TAMSAT3	2014-2014	0.0375°(~4 km)	Reading University
IMERG6	2001-2014	0.1°(~10 km)	NASA & JAXA
Streamflow data	2001-2014	Daily	EMoWI
Meteorological data	2001-2014	Daily	NMA
Land cover	2001	30*30 m	Kabite et al. (2020)
Soil map	2013/14	variable	EMoWI, FAO & OWWDSE

Shuttle Radar Thematic Mapper (SRTM) derived Digital Elevation Model (DEM) of 30*30 m spatial resolution was obtained from the United States Geological Survey (USGS). It is one of the input data for SWAT model from which topographic and drainage parameters (e.g., drainage pattern, slope and watershed boundary) were derived. Soil map was obtained from source described in Table 1. Soil physical properties required for SWAT model were derived from the soil map. Supervised image classification was used to prepare land cover map of 2001.Together with land cover and soil maps, DEM was used to create Hydrologic Response Units (HRUs).

Rainfall data for nine stations within the river basin and for three nearby stations (Figure 1), from 2001 to 2014 were obtained from the National Meteorological Agency (NMA) of Ethiopia. The rainfall data was used to evaluate the SREs using the statistical and hydrological modelling evaluation methods. In addition, Enhanced National Climate Time-series Service (ENACTS) gridded (4 m *4 m) minimum and maximum air temperature data was obtained from the National Meteorological Agency (NMA) of Ethiopia. Daily streamflow data from 2001 to 2014 was obtained for a station near the town of Arjo (Figure 1) from Ethiopian Ministry of Water, Irrigation and Energy (EMoWI).

The hydrometeorological stations used for this study were selected due to their long-term records and better data quality. The observed streamflow was used to calibrate and validate SWAT model. Land use map for 2001 and soil map were obtained from Kabite et al. (2020) and Ethiopian Ministry of Water, Irrigation and Energy (EMoWI), respectively.

2.2.1. Satellite rainfall products

The Satellite Rainfall Estimates (SREs) considered in this study include 3B42/3, TAMSAT3, CHIRPS2 and IMERG6. These datasets were selected because of several reasons including that they: i) have relatively high spatial resolution, ii) are gauge-adjusted products, iii) are the latest products and have been found to perform well by recent studies, and iv) were not compared for the basins in Ethiopia particularly IMERG6.

The TMPA provides rainfall products for area covering 50°N-50°S for the period of 1998 to present at 0.25°*0.25° and 3h spatial and temporal resolution, respectively. The 3h rainfall product is aggregated to daily (3B42) and monthly (3B43) gauge-adjusted post real time precipitation. The performance of the 3B42v7 is superior compared to its predecessor (i.e.,

3B42v6) and the real time TMPA product (3B42RT) (Yong et al., 2014). The 3B43 was used in this study for the statistical evaluation while the 3B42 was used for the hydrological performance evaluation. The detail description is given by Huffman et al. (2007).

TAMSAT3 algorithm estimates precipitation in an indirect method using cloud-index method, which compares the cold cloud duration (CCD) with predetermined temperature threshold. The CCD is the length of time that a satellite pixel is colder than a given temperature threshold. The algorithm calibrates the CCD using parameters that vary seasonally and spatially but constant from year to year. This makes interannual variations in rainfall to depend only on the satellite observation. The dataset covers the whole Africa at ~4 km and 5-day (pentadal) resolutions for the period of 1983 to present. The original 5-day temporal resolution is disaggregated to daily time-step using daily CCD from which monthly data are derived. TAMSAT3 algorithm are improved compared to its processor (i.e., TAMSAT2). The detail is described in Maidment et al. (2017).

The Climate Hazards Group InfraRed Precipitation with Stations (CHIRPS) is a quasi-global precipitation product with ~5km (0.05°) spatial resolution and is available at daily, pentadal (5-day) and monthly timescales. The CHIRPS precipitation data is available from 1981 to present. It is gauge-adjusted dataset, which is calculated using weighted bias ratios rather than using absolute station values, which minimizes the heterogeneity of the dataset (Dinku et al., 2018). The latest version of CHIRPS that uses more station data (i.e., CHIRPS version 2 here after CHIRPS2) was used in this study. Detail description of CHIRIPS2 is given in Funk et al. (2015).

The Global Precipitation Measurement (GPM) is the successor of TRMM with better rainfall detection capability. GPM provides precipitation measurements at 0.1° and half-hourly spatial and temporal resolution. Integrated Multi-satellitE Retrievals for GPM (IMERG) is one of the GPM precipitation product estimated from all constellation microwave sensors, IR-based observations from geosynchronous satellites, and monthly gauge precipitation data. IMERG is the successor algorithm of TMPA. The IMERG products includes Early Run (near real-time with a latency of 6h), Late Run (reprocessed near real-time with a latency of 18 h) and Final Run (gauge-adjusted with a latency of four months). The IMERG Final Run product provides more accurate precipitation information compared to the near-real time products as it is gauge-adjusted. The latest release of GPM IMERG Final Run version 6B (IMERG6) was used for this study. The detail is given by Huffman et al. (2014).

In this study, the performances of 3B42/3, TAMSAT3, CHIRPS2 and IMERG6 rainfall products were evaluated statistically and hydrologically. All the SREs considered in this study are gauge-corrected, and thus bias correction may not be required. Thus, rain gauge stations (e.g., Jimma and Nekemte) that were used for calibrating the SREs datasets were excluded for fair comparison. The lists of rain gauge stations used for this study are shown in Figure 1 and Appendix Table 1. The detail summaries of the data types used for this study are shown in Table 1.

2.3. Methodology

Satellite rainfall estimates offer several advantages compared to the conventional methods but can also be prone to multiple errors. Rainfall detection capability of SREs can be affected by local climate and topography (Xue et al., 2013; Meng et al., 2014). Therefore, performance of SREs should be examined for a particular area before using the products for any application (Hu et al., 2014; Toté et al., 2015; Kimani et al., 2017).

The two common SREs performance evaluation methods are statistical (i.e., ground-truthing) and hydrological modelling performance (Behrangi et al., 2011; Bitew and Gebremichael, 2011; Thiemig et al., 2013, Abera et al., 2016; Jiang et al., 2017), and were used in this study. The methods complement each other and their combined application is recommended for more reliable SREs evaluation techniques. The statistical evaluation method involves pairwise comparison of SREs and the rain gauge products. The method provides insight into the intrinsic data quality whereas the modelling approach assesses the usefulness of the data for a desired application (Thiemig et al., 2013). Statistical evaluation was performed for all the SREs products considered in this study (i.e., 3B43, CHIRPS2, TAMSAT3 and IMERG6) to examine their rainfall detection skills. Continuous and categorical validation indices were used to evaluate performance of the products. In addition, the SREs product and gauge datasets were independently used as forcing to calibrate and verify SWAT model. Accordingly, streamflow prediction performance of the rainfall products was evaluated graphically and using statistical indices.

2.3.1. Statistical evaluation of satellite rainfall estimates

Statistical SREs evaluation method was conducted at monthly, seasonal and annual timescales for the overlapping period of all the rainfall data sources (i.e., 2001-2014). A daily

comparison was excluded from this study due to weak performance reported in previous studies (Ayehu et al., 2018; Zhao et al., 2017; Li et al., 2018). This is attributed to the measurement time mismatch between ground and satellite rainfall products.

Two approaches are commonly used for the statistical evaluation method. The first approach is pixel-to-pixel pairwise comparisons of the spatially interpolated gauge-based and satellite-based data. The second approach is point-to-pixel pairwise comparison where satellite rainfall estimates are extracted for each gauge locations and the satellite-gauge data pairs are generated and compared. The second approach was used for this study. This is because the 12 rainfall stations considered in this study are unevenly distributed throughout the basin to accurately represent spatial variability of rainfall in the DRB as required for the first approach. As a result, we chose to extract gauge-satellite rainfall pair values at each rain gauge location instead of interpolating the gauge measurements into gridded products.

Accordingly, 168 and 2016 paired data points were extracted for annual and monthly analysis, respectively, and were evaluated using continuous validation indices such as Pearson correlation coefficient (r), bias ratio (*BIAS*), Nash-Sutcliffe efficiency (E) and Root Mean Square Error (*RMSE*). The Pearson correlation coefficient (r) evaluates how well the estimates correspond to the observed values; *BIAS* reflects how the satellite rainfall estimate over- or under-estimate the rain gauge observations; E shows how well the estimate predicted the observed time series. On the other hand, *RMSE* measures the average magnitude of the estimate errors. The summary of performance indices are presented in Table 2.

269 Table 2. SREs evaluation indices, mathematical descriptions and perfect score.

Indices	Mathematical expression	Description	Perfect score
Pearson correlation	$r = \frac{\sum(R_g - \overline{R_g})(R_s - \overline{R_s})}{\sqrt{\sum(R_g - \overline{R_g})^2}\sqrt{\sum(R_s - \overline{R_s})^2}}$	R_g is gauge rainfall observation; R_s satellite rainfall estimates; $\overline{R_g}$ is average gauge rainfall observation; $\overline{R_s}$ is average satellite rainfall estimates. The value ranges from -1 to 1.	1
Root mean square error (mm)	$RMSE = \sqrt{\frac{\sum(R_g - R_s)^2}{n}}$	n is the number of data pairs; the value ranges from 0 to ∞	0
Bias ratio (BIAS)	$BIAS = \frac{\sum R_s}{\sum R_g}$	A value above (below) 1 indicates an aggregate satellite overestimation (underestimation) of the ground precipitation amounts.	1
Relative bias (RB)	$RB = \frac{\sum(R_s - R_g)}{\sum R_g} * 100$	Describes the systematic bias of the SREs; positive values indicate overestimation while negative values indicate underestimation of precipitation amounts.	0
Mean Error (ME)	$ME = \frac{1}{n}\sum_{i=1}^{n}(R_s - R_g)$	Describes the average errors of the SREs relative to the observed rainfall data.	0
Nash-Sutcliffe of efficiency coefficient (E)	$E = 1 - \frac{\sum(R_s - R_g)^2}{\sum(R_g - \bar{R}_g)^2}$	The value ranges from -∞ to 1; 0<E≤1 acceptable while E≤ 0 is unacceptable	1
Probability of Detection	$POD = H/(H + M)$	H is the number of hits; M is the number of miss	1
False alarm ratio	$FAR = F/(H + F)$	F is the number of false alarms	0
Critical success index	$CSI = H/(H + M + F)$	Describe the overall skill of the satellite products relative to gauge observation.	1
Percent bias (%)	$PBIAS = \frac{\sum(Q_O - Q_s)}{\sum(Q_O)} * 100$	Q_O is observed discharge; Q_s is simulated discharge for the available pairs of data where < ±15% is very good	0
Coefficient of determination (r^2)	$r^2 = (\frac{\sum_{i=1}^{n}(O_i - \bar{O})(S_i - \bar{S})}{\sqrt{\sum_{i=1}^{n}(O_i - \bar{O})^2}\sqrt{\sum_{i}^{n}(S_i - \bar{S})^{\wedge}2}})^{\wedge}2$	O_i & $\bar{O}$ is observed & average streamflow, respectively; S_i & $\bar{S}$ is simulated and average, respectively. The value ranges from 0 to 1.	1
Nash-Sutcliffe coefficient of efficiency	$NSE = \frac{\sum(Q_o - \overline{Q_o})^2 - \sum(Q_o - Q_s)^2}{\sum(Q_o - \overline{Q_o})^2}$	$\overline{Q_o}$ is mean value of the observed discharge for the entire time under consideration	1

270 In addition to the continuous validation indices, tercile categories (i.e., percentile-based
271 evaluation) along with probability of exceedance were performed to test the performance of
272 SREs in detecting low-and high-end values. The percentile and probability of exceedance
273 methods better evaluates rainfall detection capabilities of SREs for monthly time scale
274 compared to the other categorical indices such as probability of detection (*POD*), false alarm

ratio (*FAR*) and critical success index (*CSI*). This is because the *POD*, *FAR* and *CSI* are not effective for monthly-based analysis but effective for daily-based analysis.

In general, SREs with $r>0.7$ and relative bias (*RB*) within 10% can be considered as reliable precipitation measurement sources (Brown, 2006; Condom et al., 2011). However, attention should be given to certain indices depending on the application of the product (Toté et al., 2015). For flood forecasting purpose, for example, underestimation of rainfall should be avoided (i.e., mean error (*ME*)>0 is desirable). In contrast, for drought monitoring, overestimation must be avoided (i.e., *ME*<0 is preferred) (Dembélé and Zwart, 2016).

2.3.2. SWAT model setup

Soil and Water Assessment Tool (SWAT) is a semi-distributed, deterministic and continuous simulation watershed model that simulates many water quality and quantity fluxes (Arnold et al., 2012). It is a physically based and computationally efficient model that has been widely used for various hydrological and/or environmental application in different regions of the world (Gassman et al., 2014). Furthermore, the capability of SWAT model to be easily linked with calibration, sensitivity analysis and uncertainty analysis tools (e.g., SWAT-CUP) made it more preferable.

SWAT model follows a two-level discretization scheme: i) sub-basin creation based on topographic data and ii) Hydrological Response Unit (HRU) creation by further discretizing the sub-basin based on land use and soil type. HRU is a basic computational unit assumed to be homogeneous in hydrologic response. Hydrological processes are first simulated at the HRU level and then routed at the sub-basin level (Neitsch et al., 2009). The SWAT model estimates surface runoff using the modified United States Department of Agriculture (USDA) Soil Conservation Service (SCS) curve number method. In this study, a minimum threshold area of 400 km^2 were used for determining the number of sub-basins and 5% threshold for the soil, slope, and land use were used for the HRU definition. Accordingly, 13 sub basins and 350 HRUs are created for the Arjo gauging station as outlet.

2.3.3. SWAT model calibration and validation

Hydrologic modelling performance evaluation technique is commonly performed by either calibrating the hydrologic model with gauge rainfall data and then validating with SREs,

(i.e., static parameters) or calibrating and validating the model independently with each rainfall products (i.e., dynamic parameters) and then compare accuracies of the streamflow predicted using the capacity of the rainfall products. The latter is preferred for watersheds such as the DRB where gauging stations are sparse and unevenly distributed. Moreover, studies have reported that independently calibrating the hydrologic model with SREs and gauge data improves performance of the hydrological model (Zeweldi et al., 2011; Vernimmen et al., 2012; Lakew et al., 2017).

Calibration, validation and sensitivity analysis of SWAT was done using the SWAT-CUP software. The Sequential uncertainty fitting (SUFI-2) implemented in SWAT-CUP was used in this study (Abbaspour et al., 2007). SUFI-2 provides more reasonable and balanced predictions than the generalized likelihood uncertainty estimation (GLUE) and the parameter solution (ParaSol) methods (Zhou et al., 2014; Wu and Chen et al., 2019) offered by the tool. It also estimates parameter uncertainty attributed to input data, and model parameter and structure as total uncertainty (Abbaspour, 2015). The total uncertainty in the model prediction is commonly measured by P-factor and *R*-factor. *P*-factor represents the percentage of observed data enveloped by the 95 percent prediction uncertainty (95PPU) simulated by the model. The *R*-factor represents the ratio of the average width of the 95PPU band to the standard deviation of observed data. For realistic model prediction, *P*-factor $\geq$0.7 and *R*-factor $\leq$1.5 is desirable (Abbaspour et al., 2007, Arnold et al., 2012).

The first steps in SWAT model calibration and validation process is determining the most sensitive parameters for a given watershed. For this study, 19 parameters were identified based on the recommendations of previous studies (Roth et al., 2018; Lemann et al., 2019). Global sensitivity analysis was performed on the 19 parameters from which 11 parameters were found sensitive for the DRB, and were used for calibration, verification, and uncertainty analysis. The hydrologic simulations were performed for the 2001 to 2014 period. Two years of spin-up (warm-up) period (i.e., 2001 and 2002), and 6 years of calibration period (2003 to 2008), and 6 years of verification periods (2009 to 2014) were used. Graphical and statistical measures were used to evaluate prediction capability of the rainfall datasets. Accordingly, the performance of model forced by each rainfall datasets was tested using the most widely used statistical indices (i.e., R^2, *NSE* and *PBIAS*), in addition to the *P*-factor and *R*-factor.

3. Results

3.1. Statistical evaluation

Figure 2 compares mean annual spatial rainfall distributions of the DRB. Average annual rainfall of the study area for the 2001 to 2014 period was 1682.09 mm/year (1150 to 2127 mm/year), 1698.59 mm/year (1432 to 1837 mm/year), 1699.06 mm/year (1092 to 2414 mm/year) and 1680.28 mm/year (1342 to 1721 mm/year) according to the CHIRPS2, IMERG6, TAMSAT3 and 3B43 products, respectively. For reference, mean annual rainfall for the DRB is 1650 mm/year based on the rain gauge data, which is within 1.8% to 3% of the estimates provided by the products. However, total annual rainfall range estimates were substantially different among the products. The decreasing rainfall trend from the southern (highlands) to the northern (lowlands) part of the basin were captured by all products. In particular, TAMSAT3 and CHIRPS2 captured the rainfall variability in better detail, perhaps due to their high spatial resolution. On the other hand, resolution of the 3B43 rainfall product seems too coarse to satisfactorily represent spatial variability of rainfall in the basin.

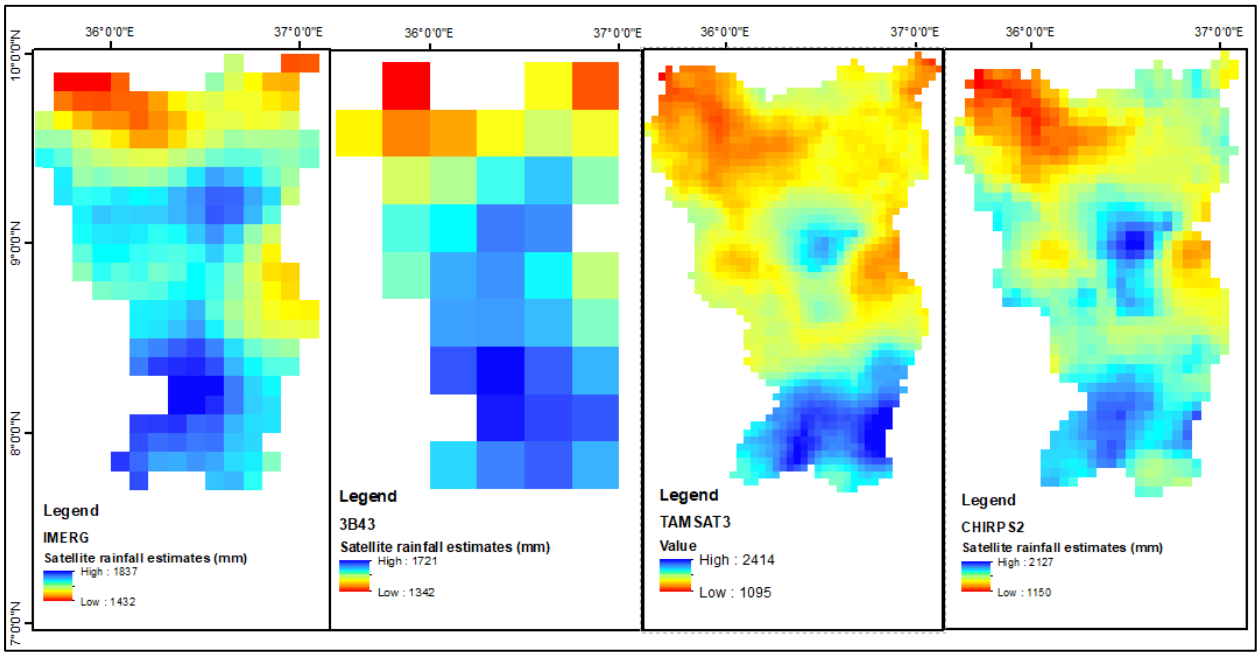

Figure 2. Spatial mean annual rainfall distribution of the four SREs for DRB (2001 to 2014)

Figures 3 to 5 show results of statistical evaluation indices calculated from rainfall from the rain gauges and from the SREs products. More specifically, Figures 3 and 4 show correlation coefficients for the annual and monthly timescales, respectively. The results show that all four SREs products produced rainfall that correlate better to the ground based rainfall

observations at monthly timescale than at annual time scales. This is because performance of SREs improved with increased time aggregation and peaks at monthly timescale. More likely, the seasonal variability is much larger than the interannual variability. The seasonal variability is, apparently, captured reasonably well, causing a higher degree of correlation for monthly data. The values of statistical evaluation indices for all products are summarized in Table 3. The results show that the CHIRPS2 performed better for the DRB with relatively higher *r* and *E*, and lower *BIAS*, *ME* and *RMSE* for annual and monthly timescales, respectively.

Table 3. Statistical evaluation indices of all SREs.

	R		*BIAS*		*ME*		*RMSE* (mm)		*E*	
SREs	Annual	Monthly	Annual	Monthly	Annual	Monthly	Annual	Monthly	Annual	Monthly
CHIRPS2	0.78	0.92	1.01	1.01	25.94	2.70	214.36	50.48	0.51	0.84
3B43	0.48	0.87	1.02	1.02	30.58	2.55	306.34	62.05	0.76	0.76
IMERG6	0.52	0.90	1.03	1.03	48.87	4.07	299.55	56.95	0.39	0.80
TAMSAT3	0.62	0.89	1.03	1.03	51.46	2.67	274.00	61.28	0.77	0.77

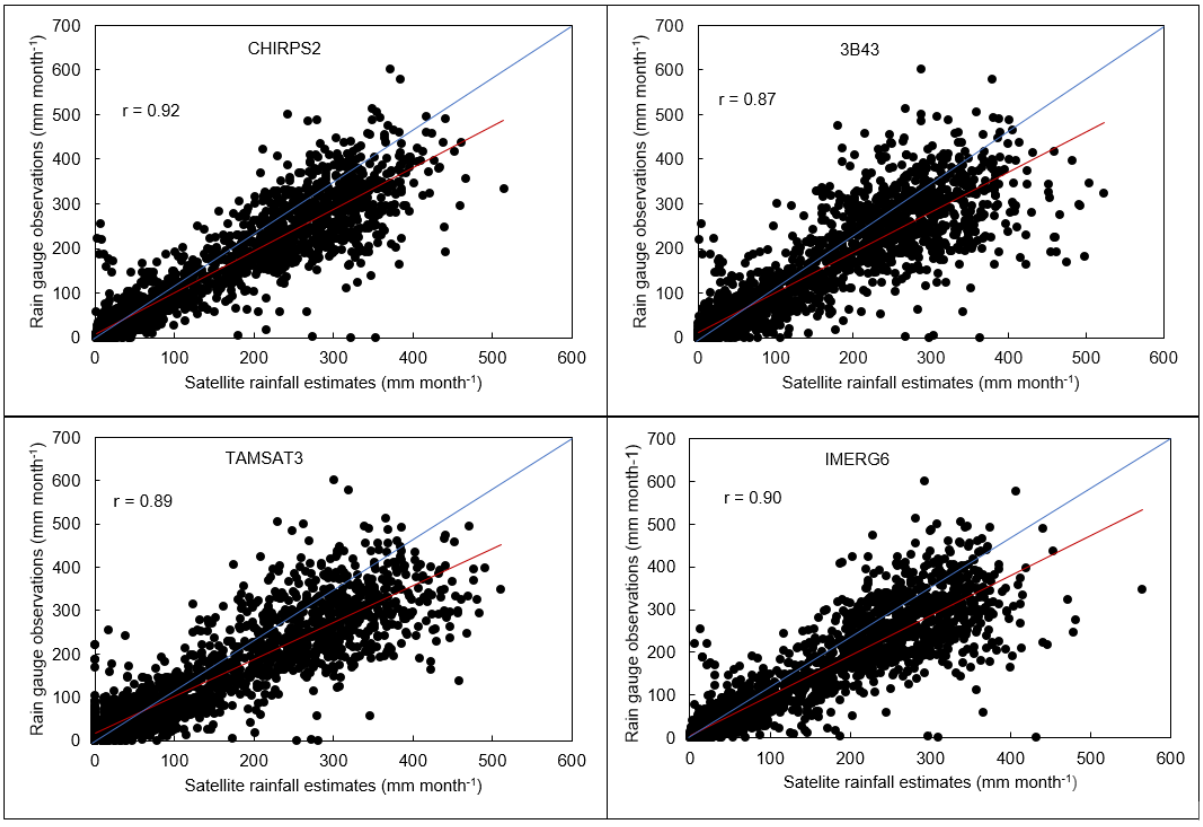

Figure 3. Correlation coefficient of the four SREs at monthly timescale over DRB.

Figures 3 to 5 and Table 3 show that generally, CHIRPS2 performed better than the other three products for the DRB. Correlation coefficients for both monthly and annual

timescales as well as all the indices presented in Figure 5 favor CHIRPS2 indicating its superior performance. Relative performance of the other three SREs is inconsistent as it varies with the statistical indices used in this study. The 3B43 product, for example, performed worse based on Figure 3 and 4 (i.e., correlation coefficients for annual and monthly timescales) and *RMSE* and *E* (Figure 5), but performed better than the other two SREs based on *BIAS* and *ME*.

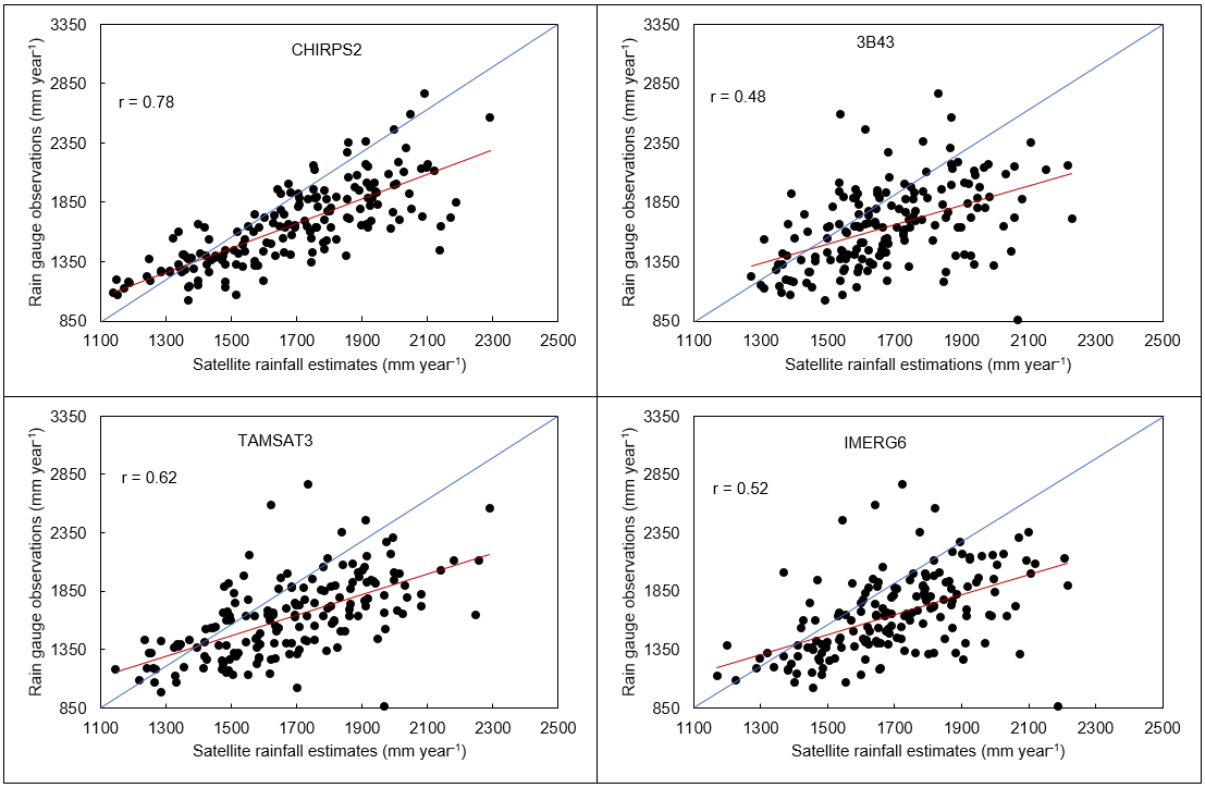

Figure 4. Annual correlation coefficient of the four SREs for the DRB.

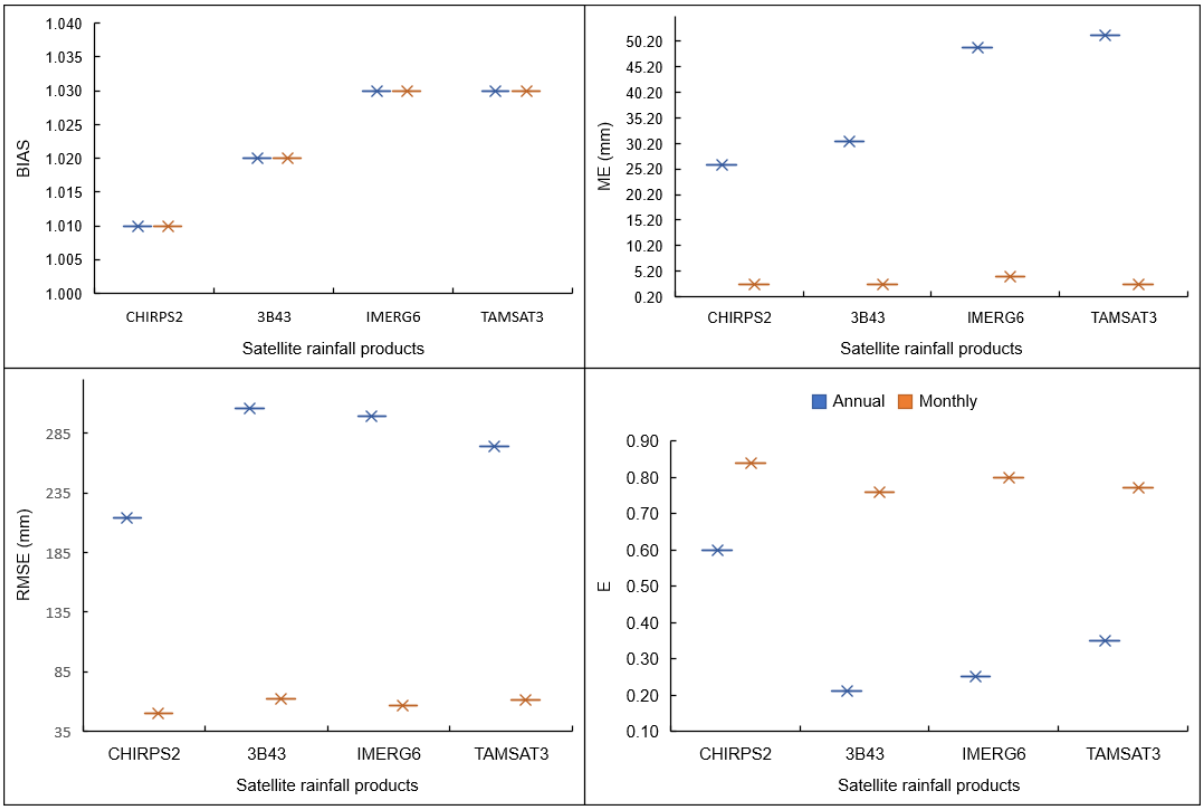

Figure 5. Statistical indices of the four SREs for DRB at annual and monthly time scales.

Tercile (percentile) categorical and probability of exceedance analysis result (Figure 6) show that all the SREs considered in this study have high rainfall detection capability for the DRB. Rainfall threshold used for this figure is 1mm/day. The lower tercile (33th *percentile;* P33), middle tercile (67th *percentile;*P67*)* and higher tercile (100th *percentile;*P100) of all SREs closer values with the corresponding gauge values indicating that the SREs detects rainfall for the DRB. Moreover, the probability of exceedance further confirms the rainfall detection capability of the SREs considered in this study for the DRB. However, TAMSAT3 exhibited relatively less rainfall detection skill, which could be attributed to the relatively more sensitivity of TAMSAT3 to topographic effects.

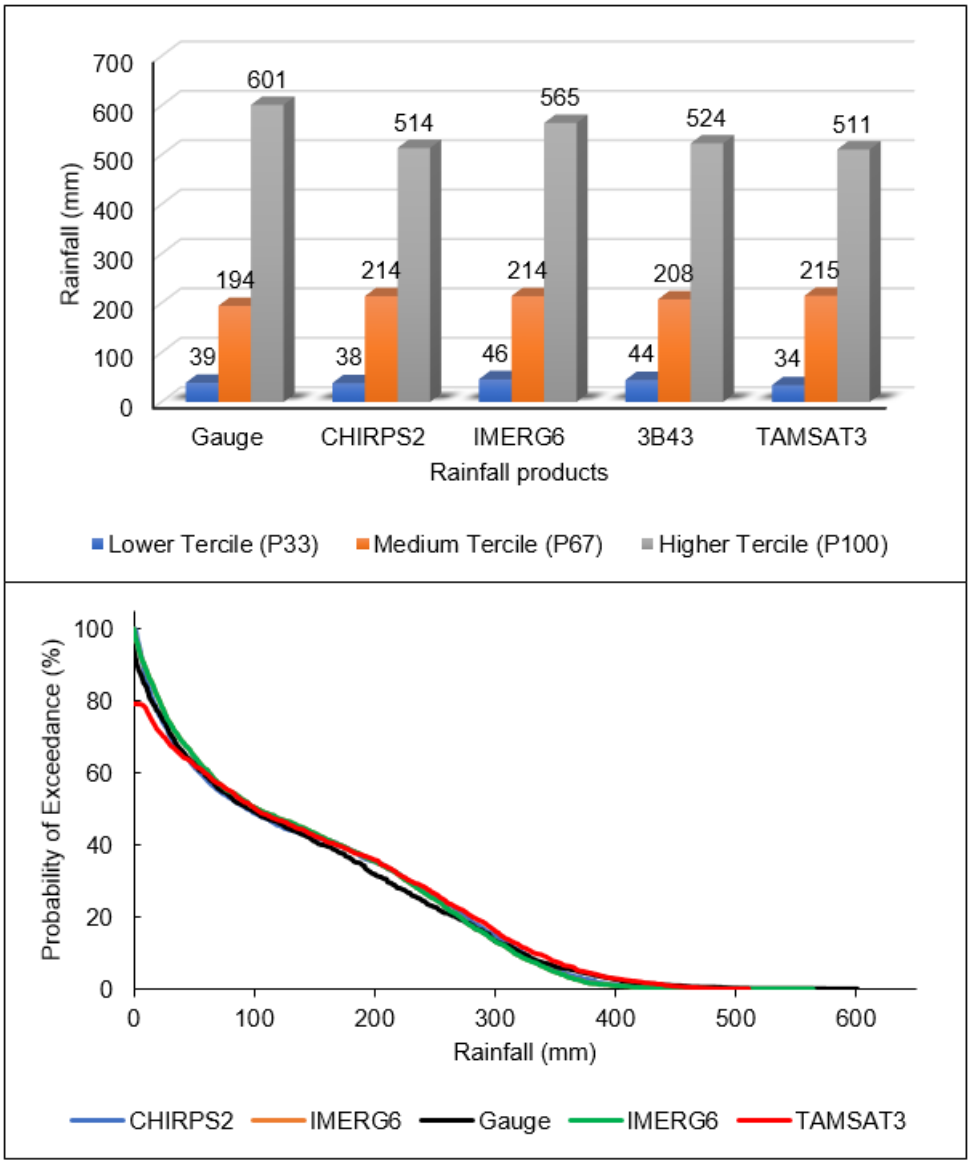

Figure 6. Tercile categories (top) and probability of exceedance of SREs.

Figure 7 shows seasonal SREs performance evaluation results. The figure generally shows that performance of the SREs varied from season to season and among the rainfall products. Main rainy season in the DRB is from June to September while short rainy season ranges from March to May but the rest is dry season (Figure 9). For example, CHIRPS2 is superior in detecting and estimating rainfall events for the DRB for all months (seasons). The rainfall detection and estimating capability of CHIRPS2 is better for rainy season compared to the dry season. Likewise, the rainfall detection capability of TAMSAT3 is stronger for the rainy season (May to November) but weaker for the dry season (December to April). Compared to the other SREs products, TAMSAT3 generally poorly correlated for all months (seasons), and its *BIAS* was the highest for rainy season but the lowest for the dry season.

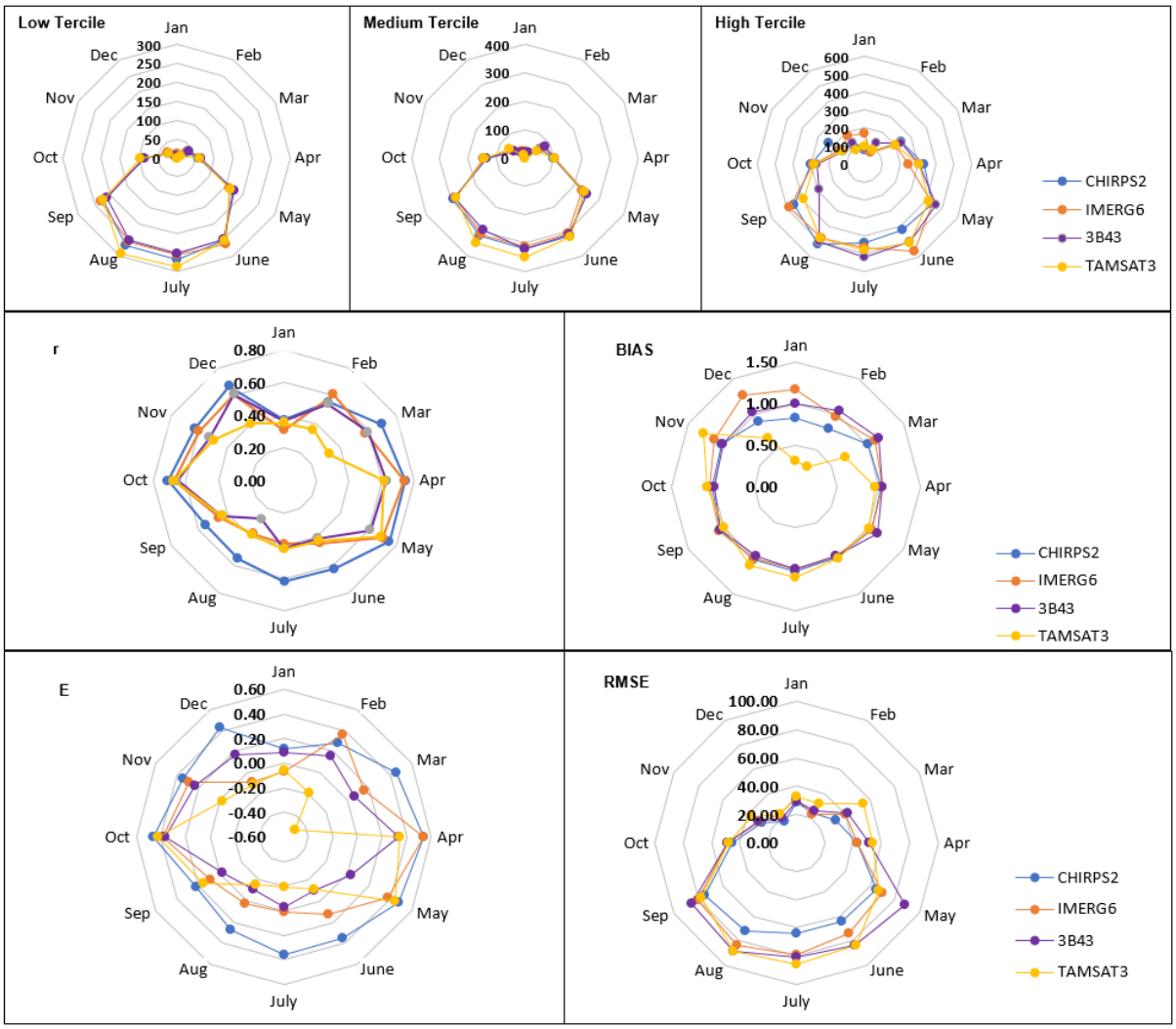

Figure 7. Seasonal statistical evaluation result comparison of each SREs for the DRB.

3.2. Hydrological modelling performance evaluation

The centroid of each sub basins were used as gauging locations, and used for extracting rainfall for all the SREs rainfall datasets. Thus, each sub basins are represented by a separate and dense gauges unlike that of the measured rainfall representation. The performance of the rainfall products were evaluated using SWAT-CUP at monthly time steps.

Table 4 shows details of the calibrated parameters including their ranges, best fit values, sensitivity ranks when different rainfall datasets are used as inputs for the DRB. The best fit values were multiplied by (1+ given value) and replaced by the given value for the parameters with *r*-prefix and *v*-prefix, respectively. The table shows that ranges and the best fit values vary from rainfall data source to another. This indicates the sensitivity of hydrological model performance to rainfall products and thus accurate characterization of rainfall variability is very

critical for reliable hydrological predictions. This finding is consistent with studies that reported that different precipitation datasets influence model performance, parameter estimation and uncertainty in streamflow predictions (Sirisena et al., 2018; Goshime et al., 2019). Relative sensitivity of the parameters also varied between the rainfall datasets. In general, threshold depth of water in the shallow aquifer required for return flow to occur (mm) (*GWQMN.gw)*, base flow alpha factor *(ALPHA_BF.gw)*, Groundwater delay (day) *(GW_DELAY.gw)*, deep aquifer percolation fraction *(RCHRG_DP.gw)*, and runoff curve number for moisture condition II *(CN2.mgt)* are top five sensitive parameters. This seems indicate that groundwater processes dominate streamflow in the DRB. This could be attributed to the dominantly deep and permeable soil, vegetated land surface and dominant tertiary basaltic rocks in the DRB (Conway, 2000; Kabite and Gessesse, 2018). The groundwater parameters can have a strong effect on the amount of streamflow that can cause over or underestimation of streamflow. For this reason, the validation of streamflow was sorely dependent on the rainfall products.

Table 4. Initial parameter ranges, fit values, and sensitivity ranks for rainfall data sources.

	Initial values	Gauge		CHIRPS2		IMERG6		3B42		TAMSAT3	
Parameters		Fit value	Rank	Fit value	Rank	Fit value	Rank	Fit value	Rank	Fit value	Rank
v_GWQMN.gw	0 to 5000	4936.02	1	201.64	3	3379.76	3	4784.74	1	-0.15	1
v_ALPHA_BF.gw	0 to 1	0.00	2	0.45	4	0.04	4	0.00	2	0.00	2
v_GW_DELAY.gw	0 to 500	339.10	3	29.02	5	34.76	6	391.13	4	318.08	3
v_RCHRG_DP.gw	0 to 1	0.02	4	0.44	7	0.04	5	0.30	3	0.04	4
r_CN2.mgt	-0.25 to 0	310.12	5	-0.25	11	-0.17	10	-0.13	5	-0.15	5
r_SOL_K.sol	0 to 2000	260.96	6	1086.63	9	391.90	11	286.12	6	447.41	6
v_CH_N2.rte	-0.01 to 0.3	0.74	7	0.02	1	0.05	1	0.29	8	0.61	7
v-CH_K2.rte	-0.01 to 500	310.12	8	354.51	2	426.08	2	256.15	7	298.36	8
v_GW_REVAP.gw	0.02 to 0.2	0.40	9	0.15	8	0.20	8	0.26	9	0.33	10
r_SOL_AWC.sol	-0.5 to 0.5	-0.01	10	-0.49	6	-0.19	7	-0.85	10	-0.59	9
v_REVAPMN.gw	0 to 500	170.26	11	14.52	10	381.84	9	142.11	11	176.48	11

Figure 8 compares the observed and the predicted streamflows for the calibration (2003 to 2008) and verification (2009 to 2014) periods for all five rainfall datasets. Goodness of the streamflow predictions is also summarized in Table 5. The results show that the peak streamflow is underestimated for all rainfall products, including gauges, but the streamflow volume is generally overestimated. This could be due to the uncertainity of SREs for the extreme rainfall events at daily scale (Jiang et al., 2017) and SWAT model error. The overestimated streamflows could also be attributed to overestimation of rainfalls by the SREs

as described in the previous sections. Generally, the indices provided in Table 4 indicate that the streamflow predictions are good for CHIRPS2, IMERG6, and satisfactory for the gauged rainfall but not for TAMSAT3 and 3B42 according to Moriasi et al. (2017) classification system. The performance of the SREs are consistent with the climatology of the products. Mean monthly rainfall from 2001 to 2014 showed that TAMSAT3 and 3B42 deviate more from observed rainfall while CHIRPS2 and IMERG6 are relatively closer (Figure 9).

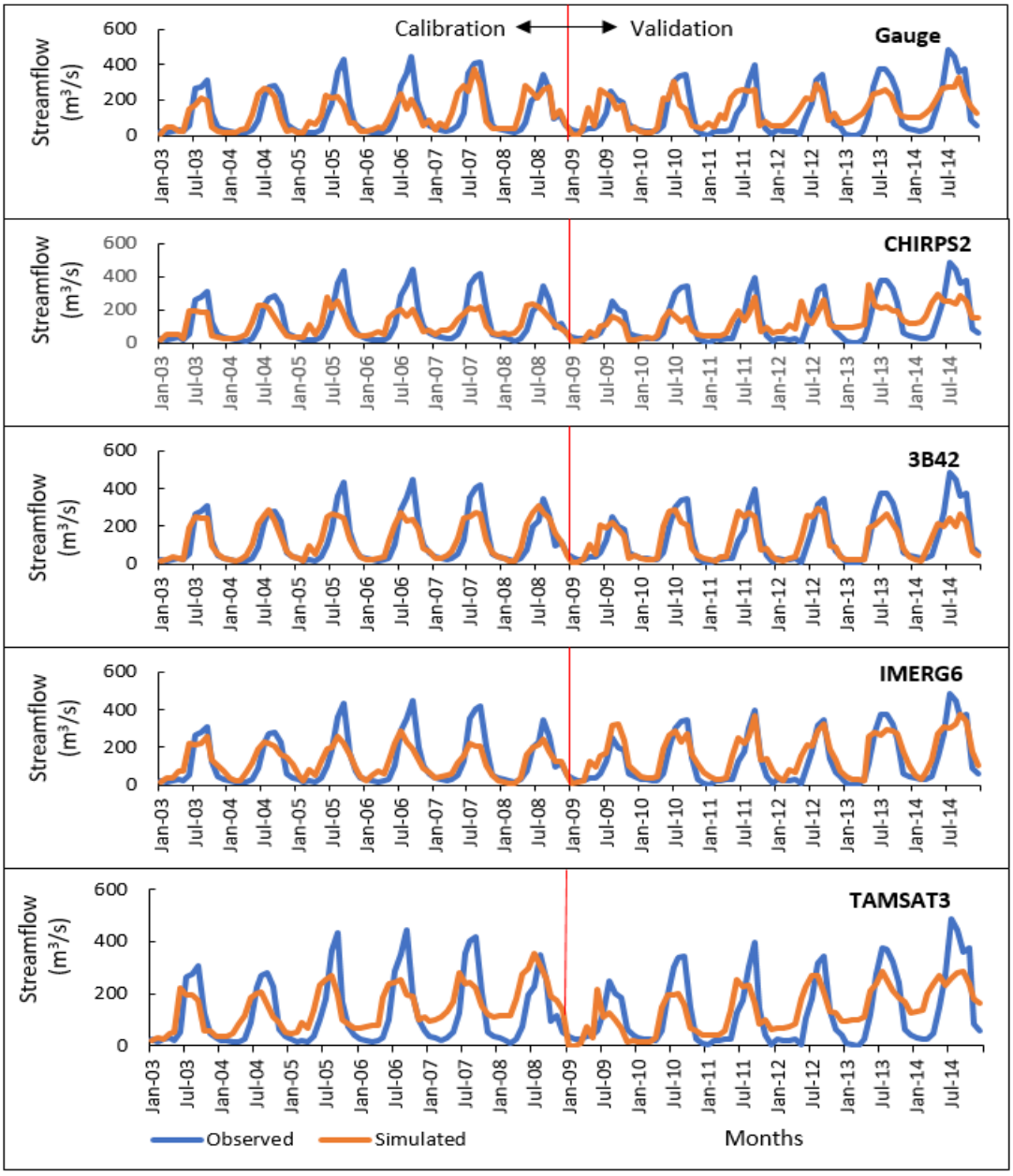

Figure 8. Graphical calibration and validation of streamflow at monthly scale.

Table 5. Calibration and validation results for the different rainfall products.

Rainfall products	Calibration					Validation				
	NSE	R^2	*PBIAS*	*P*-factor	*R*-factor	*NSE*	R^2	*PBIAS*	*P*-factor	*R*-factor
Gauge	0.55	0.54	2.8	0.43	0.55	0.54	0.57	-9.3	0.15	0.27
CHIRPS2	0.69	0.7	-2.5	0.72	0.64	0.65	0.66	5.3	0.46	0.58
IMERG6	0.65	0.67	2.2	0.70	0.66	0.73	0.78	-14.5	0.64	0.86
TAMSAT3	0.43	0.46	-16.7	0.31	2.94	0.48	0.48	-4.9	0.46	2.68
3B42	0.48	0.51	8.6	0.65	3.88	0.45	0.46	1.3	0.82	2.96

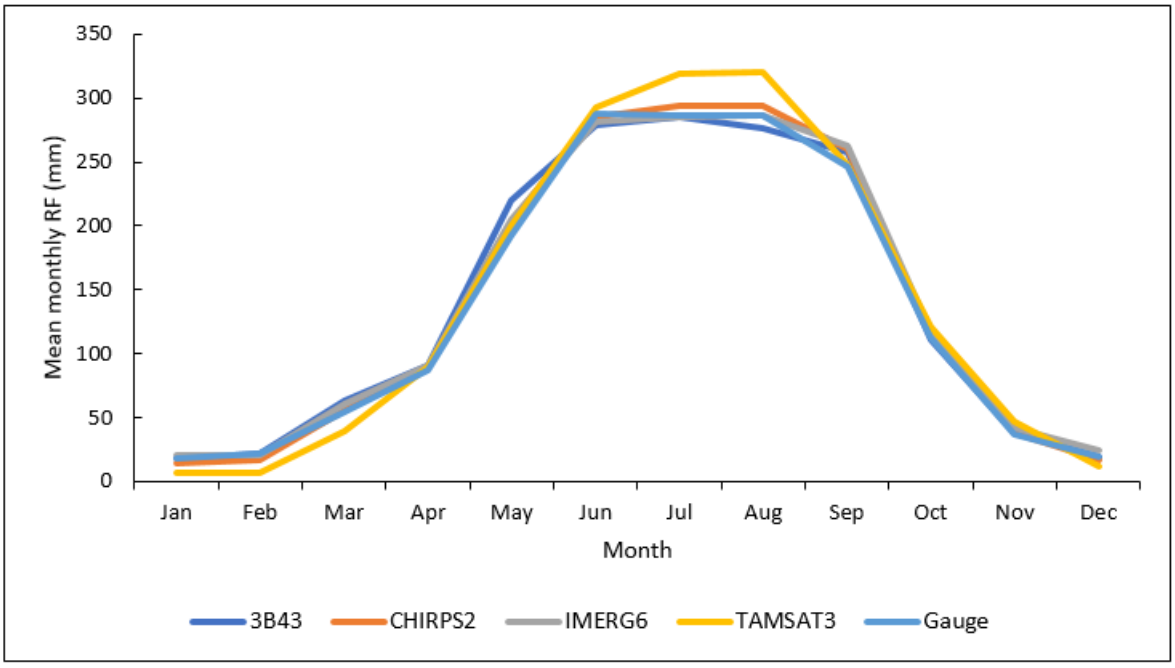

Figure 9. Mean monthly rainfall (2001 to 2014).

4. Discussion

The statistical SREs evaluation result showed that all the rainfall products captured the spatiotemporal rainfall variability of the DRB except the 3B43. Poor performance of 3B43 in capturing basin's rainfall variability is in agreement with findings of two previous studies done for other basins in Ethiopia (Dinku et al., 2008; Worqlul et al., 2014). The reasons could be attributed to the fact that gauge adjustment for 3B43 product did not use adequate gauge data from Ethiopian highlands due to lack of data (Haile et al., 2013) and coarse spatial resolution of the dataset (Huffman et al., 2007). However, Gebremicael et al. (2019) reported better performance of 3B43 for the Tekeze-Atibara basin, which is located in the northern mountainous area of Ethiopia.

Better correlation of SREs with observed rainfall was observed at monthly than at annual timescales for all products. This is consistent with studies that reported the performance of SREs improved with increased time aggregation that peaks at monthly timescale (Dembélé and Zwart, 2016; Katsanos et al., 2016*;* Zhao et al., 2017; Ayehu et al., 2018; Li et al., 2018; Guermazi et al., 2019). The weak agreement of SREs with observed data at annual timescale shows that the SREs considered in this study generally did not capture the interannual rainfall variability. In this regards, particularly the 3B43 product failed to capture annual rainfall variability compared to the other three SREs. Overall, all four SREs products overestimated rainfall for the DRB by 10% for CHIRPS2 to 30% for IMERG6 and TAMSAT3 (Figure 5). This finding is consistent with studies that reported overestimation of IMERG6 and 3B43 products for the alpine and gorge regions of China (Chen et al., 2019). However, Gebremicael et al. (2019) reported underestimation of rainfall by CHIRPS2 for the Tekeze-Atbara basin, which is a mountainous and arid basin in northern Ethiopia. Ayehu et al. (2018) also reported slight underestimation of rainfall by CHIRPS2 for the upper Blue Nile Basin. The discrepancy between our finding and the previous studies done for the basins in Ethiopia may be due to differences in watershed characteristics such as topography, vegetation cover and climatic conditions.

Generally, this study showed that the SREs products considered in this study exhibited satisfactory rainfall detection and estimation capability for the DRB. The products could be applicable for flood forecasting applications for the DRB *(*Toté et al., 2015*)*. CHIRPS2 performed better than the other three SREs for annual, seasonal, and monthly timescales in detecting and estimating rainfall for the basin. The superiority of CHIRPS2 was also reported by previous studies for different parts of world (Katsanos et al., 2016; Dembélé and Zwart, 2016*)* including basins in Ethiopia (Bayissa et al., 2017; Ayehu et al., 2018; Dinku et al., 2018; Gebremicael et al., 2019). For example, Dinku et al. (2018) reported better rainfall estimation capability of CHIRPS2 for East Africa compared to African Rainfall Climatology version 2 (ARC2) and TAMSAT3 products. Ayehu et al. (2018) reported better performance of CHIRPS2 for the Blue Nile Basin compared to ARC2 and TAMSAT3. Better performance of CHIRPS2 has been attributed to the capability of the algorithm to integrate satellite, gauge and reanalysis products and its high spatial and temporal resolution (Funk et al., 2015). On the contrary, generally, the 3B43 rainfall product performed poorly for the DRB for all timescales. This could be due to its coarse spatial resolution and lack of gauge-adjustment for highlands of Ethiopia (Haile et al., 2013). The IMERG6 showed better rainfall detection and estimation

capability for the study area than the 3B43 product, which is consistent with findings of previous studies (Huffman et al., 2015; Zhang et al., 2018; Zhang et al., 2019). Better performance of IMERG6 is attributed to the inclusion of dual and high-frequency channels, which improve light and solid precipitation detection capability (Huffman et al., 2015).

Hydrologic simulation performance evaluation result of SREs showed that accurate characterization of rainfall variability is very critical for reliable hydrological predictions. This finding is consistent with studies that reported that different precipitation datasets influence model performance, parameter estimation and uncertainty in streamflow predictions (Sirisena et al., 2018; Goshime et al., 2019). Overestimation of streamflow for all SREs products could be resulted from uncertainty of SREs for extreme rainfall events at daily scale (Zhao et al., 2017). The overestimated streamflow could also be attributed to overestimation of rainfalls by the SREs as described in the previous sections and uncertainity of SWAT model.

Overall, this study showed that CHIRPS2 and IMERG6 predicted streamflow better than the gauge rainfall and other two SREs products for the DRB. Superior hydrological performance of SREs products compared to gauge rainfall data were also reported by many other studies (Grusson et a., 2017; Bitew and Gebremichael, 2011; Goshime et al., 2019; Xian et al., 2019; Li et al., 2018; Belete et al., 2020). For example, Bitew and Gebremichael (2011) reported that satellite-based rainfall predicted streamflow better than gauge rainfall for complex high-elevation basin in Ethiopia. Likewise, a bias-corrected CHIRP rainfall dataset resulted in better streamflow prediction than a gauge rainfall dataset for Ziway watershed in Ethiopia (Goshime et al., 2019).

The relatively poor performance of gauge rainfall compared to the CHIRPS2 and IMERG6 shows that the existing rainfall gauges do not represent spatiotemporal variability of rainfall in the DRB. The rain gauges are sparse, spatially uneven, and incomplete records for the DRB. As previously mentioned, rain gauge density for the DRB is 0.32 per 1000 km^2, which is much lower than the World Meteorological Organization (WMO) recommendation of one gauge per 100-250 km^2 for mountainous areas of tropical regions such as the DRB (WMO, 1994).

In contrast to several previous studies on SREs evaluation, the present study combined statistical and hydrological performance evaluation in data scarce river basin of upper Blue Nile basin, the Dhidhessa River Basin. This method is important to identify SREs that better

519 detect and estimate rainfall, and select application specific rainfall products such as for
520 hydrologic and climate change studies. The results of this study also highlights seasonal
521 dependence of rainfall detection and hydrologic performance capability of SREs for DRB and
522 similar basins in Ethiopia. In addition, the performance of IMERG6, which is the latest SREs
523 product, was evaluated for Ethiopian basin for the first time. Overall, this study showed that
524 CHIRPS2 and IMERG6 rainfall products performed best in terms of detecting and estimating
525 rainfall as well as predicting streamflow for the DRB.

526 **5. Conclusions**

527 Satellite rainfall estimate is an alternative rainfall data source for hydrological and
528 climate studies for data scarce regions like Ethiopia. However, SREs contain uncertainties
529 attributed to errors in measurement, sampling, retrieval algorithm and bias correction
530 processes. Moreover, the accuracy of rainfall estimation algorithm is influenced by topography
531 and climatic conditions of a given area. Therefore, SREs products should be evaluated locally
532 before they are used for any application. In this study, we examined the intrinsic data quality
533 and hydrological simulation performance of CHIRPS2, IMERG6, 3B42/3 and TAMSAT3
534 rainfall datasets for the DRB. The statistical evaluation results generally revealed that all four
535 SREs products showed promising rainfall estimation and detection capability for the DRB.
536 Particularly, all SREs captured the south-north declining rainfall patterns of the study area.
537 This could be due to the fact that all the SREs products were gauge adjusted and that they are
538 the latest and improved versions. However, all the SREs datasets overestimated rainfall for
539 DRB indicating that the rainfall products could be applicable for flood studies but not for
540 drought studies. The result also showed strong correlation of all SREs with measured rainfall
541 data for the monthly timescales than for the annual timescales, which shows that all the rainfall
542 products considered in this study cannot capture interannual rainfall variability.

543 The quantitative statistical indices showed that CHIRPS2 performed the best in
544 estimating and detecting rainfall events for the DRB at monthly as well as annual timescales.
545 This is likely due to the fact that CHIRPS2 was developed by merging satellite, reanalysis and
546 gauge datasets at high spatial resolution whereas 3B43 performed poorly for the basin.

547 The hydrological modelling based performance evaluation showed that ranges, best fit
548 values, and relative sensitivities of SWAT's calibration parameters varied with the rainfall
549 datasets. Overall, groundwater flow related parameters such as *GWQMN.gw, ALPHA_BF.gw,*

GW_DELAY.gw and *RCHRG_DP.gw* were found more sensitive for all rainfall products. This showed that subsurface processes dominate hydrologic response of the DRB. The hydrological simulation performance results also showed that all the rainfall products, including the observed rainfall, overestimated streamflow especially the high flows. The peak streamflow overestimation could be attributed to the uncertainty of SREs rainfall to predict at shorter timescale (e.g., daily) and event rainfalls. The study showed CHIRPS2 and IMERG6 predicted streamflow for the basin satisfactorily, and even outperformed performance of the gauge rainfall. The relatively poor performance of the gauge rainfalls can be attributed to the fact that the gauges are too sparse to accurately characterize rainfall variability in the basin. Overall, CHIRPS2 and IMERG6 products seem to perform better for the DRB to detect rainfall events, to estimate rainfall quantity, and to improve streamflow predictions. The new insights of this study include: i) the SREs evaluation was done by combining statistical and hydrological modelling methods; ii) the SREs considered in this study are the latest products reported best in different studies, and IMERG6 is the most recent product evaluated in Ethiopian basin's for the first time in this study and iii) the rainfall detection and estimation as well as streamflow prediction capability of SREs is dependent on seasons. The results of this study are of interest to both scientific communities and water resource managers, and this paper has made a good contribution to improve understanding of the latest SREs for Ethiopia and the DRB. However, streamflow simulation capability of the selected SREs products may be tested for other hydrologic model to see if model types affect the results.

Funding: This research did not receive any specific grant from funding agencies in the public, commercial, or not-for-profit sectors.

Supplementary Materials: Provided up on request.

Author contributions

Gizachew Kabite: Conceptualization, Data collection, analysis and interpretation, writing-original draft preparation.

Misgana K. Muleta and Berhan Gessesse: Writing-review and editing. All authors have read and agreed to the published version of the manuscript:

Conflicts of Interest

The authors declare no conflict of interest.

Acknowledgments

We are grateful to the Ethiopian Space Science and Technology Institute for providing partial financial support for this research. We are also thankful to the developers of CHIRPS2, IMERG6, TAMSAT3 and 3B42 datasets and for providing the data free of charge. The National Meteorological Agency of Ethiopia and the Ethiopian Ministry of Water, Irrigation and Energy are also acknowledged for providing climate and streamflow data, respectively.

References

Abbaspour, K.C.: SWAT-CUP 2012: SWAT Calibration and Uncertainty Programs-A User Manual; Swiss Federal Institute of Aquatic Science and Technology: Eawag, Switzerland. 2015.

Abbaspour, K.C., Yang, J., Maximov, I., Siber, R., Bogner, K., Mieleitner, J., Zobrist, J., and Srinivasan, R.: Modelling hydrology and water quality in the pre-alpine/alpine watershed using SWAT, J. Hydrol. 333, 413-430, 2007.

Abera, W., Brocca, L., and Rigon, R.: Comparative evaluation of different satellite rainfall estimation products and bias correction in the Upper Blue Nile (UBN) basin, Atmos. Res. 178-179,471-483, 2016.

Arnold, J.G., Moriasi,D.N., Gassman, P.W., K.C. Abbaspour, M.J. White, R. Srinivasan, C. Santhi, R.D. Harmel, A. Van Griensven, M.W., and Liew, V.: SWAT: Model use, calibration, and validation, Trans. ASABE. 55, 1491-1508, 2012.

Ayehu, G.T., Tadesse, T., Gessesse, B., and Dinku, T.: Validation of new satellite rainfall products over the Upper Blue Nile Basin, Ethiopia, Atmos. Meas. Tech. 11, 1921-1936, 2018.

Bayissa, Y., Tadesse, T., Demisse, G., and Shiferaw, A.: Evaluation of satellite-based rainfall estimates and application to monitor meteorological drought for the Upper Blue Nile Basin, Ethiopia, Remote Sens. 9,669, 2017.

Behrangi, A., Khakbaz, B., Jaw,T. Ch., Kouchak, A. A., Hsu, K. and Sorooshian, S.: Hydrologic evaluation of satellite precipitation products over a mid-size basin, J. Hydrolo. 397,225-237, 2011.

609 Belete, M., Deng, J., Wang, K., Zhou, M., Zhu, E., Shifaw, E., and Bayissa, Y.: Evaluation
610 of satellite rainfall products for modeling water yield over the source region of Blue
611 Nile Basin, Sci. Total Environ. 708,134834, 2020.
612 Berne, A., and Krajewski, W.F.: Radar for hydrology: Unfulfilled promise or
613 unrecognized potential? Adv. Water Resour. 51, 357-366, 2013.
614 Bitew, M.M., and Gebremichael, M.: Evaluation of satellite rainfall products through
615 hydrologic simulation in a fully distributed hydrologic model, Water Resour. Res. 47,
616 1-11, 2011.
617 Brown, J.E.M.: An analysis of the performance of hybrid infrared and microwave satellite
618 precipitation algorithm over India and adjacent regions. Remote Sens, Environ. 101,
619 63-81, 2006.
620 Chen, J., Wang, Z., Wu, X., Chen, X., Lai, C., and Zeng, Z., Li, J.: Accuracy evaluation of
621 GPM multi-satellite precipitation products in the hydrological application over alpine
622 and gorge regions with sparse rain gauge network. Hydrol. Res. 50, 6, 2019.
623 Condom, T., Rau, P. and Espinoza, J. C.: Correction of TRMM 3B43 monthly
624 precipitation data over the mountainous areas of Peru during the period 1998-2007,
625 Hydrol. Process. 25, 1924-1933, 2011.
626 Conway, D.: The Climate and Hydrology of the Upper Blue Nile River, The Geogr. J. 1, 49-
627 62, 2000.
628 Dembélé, M., and Zwart,S, J.: Evaluation and comparison of satellite-based rainfall
629 products in Burkina Faso, West Africa, Int. J. Remote Sens. 37(17), 3995-4014, 2016.
630 de Goncalves, L.G.G., Shuttleworth, W.J., Nijssen, B., Burke, E.J., Marengo, J.A., Chou, S.C.,
631 Houser, P., and Toll, D.L.: Evaluation of model-derived and remotely sensed
632 precipitation products for continental South America, J. Geoph. Res, 111: D16113,
633 2006.
634 Dinku, T., Chidzambwa, S., Ceccato, P., Connor, S. and Ropelewski, C.: Validation of
635 highresolution satellite rainfall products over complex terrain, Int. J. Remote Sens.,
636 29, 4097-4110, 2008.
637 Dinku, T., Funk, C., Peterson, P., Maidment, R., Tadesse, T., Gadain, H., and Ceccato., P.:
638 Validation of the CHIRPS satellite rainfall estimates over eastern Africa, Quar. J.
639 Roy. Meteo. Soci. 144, 292-312, 2018.
640 Dinku, T., Ruiz, F., Connor, S.J. and Ceccato, P.: Validation and Intercomparison of
641 Satellite Rainfall Estimates over Colombia, J. Appl. Meteorol. Climatol. 49, 1004-
642 1014, 2010.

643 Funk, C., Verdin, A., Michaelsen, J., Peterson, P., Pedreros, D. and Husak, G.: A global
644 satellite-assisted precipitation climatology, Earth Syst. Sci., Data. 7, 275-287, 2015.
645 Gassman, P.W., Sadeghi, A.M., and Srinivasan, R.: Applications of the SWAT model
646 special section: Overview and insights, J. Environ. Qual. 43, 1-8, 2014.
647 Gebremicael, T.G., Mohamed, Y.A., van der Zaag, P., Gebremedhin, M., Gebremeskel, G.,
648 Yazew, E., and Kifle, M.: Evaluation of multiple satellite rainfall products over the
649 rugged topography of the Tekeze-Atbara basin in Ethiopia, Int. J. Remote Sen.
650 40(11), 4326-4345, 2019.
651 Gebremichael, M., Bitew, M.M., Hirpa, F.A., and Tesfay, G. N.: Accuracy of satellite
652 rainfall estimates in the Blue Nile Basin: Lowland plain versus highland mountain,
653 Water Resour. Res. 50, 8775-8790, 2014.

654 Geological Survey of Ethiopia (GSE): Geology of the Nekemte and Gimbi Area. Sheet
655 Number: NC-37-9 and NC-36-12, respectively. Unpublished, 2000.

656 Goshime, D.W., Absi, R., and Ledésert, B.: Evaluation and Bias Correction of CHIRP
657 Rainfall Estimate for Rainfall-Runoff Simulation over Lake Ziway Watershed,
658 Ethiopia, Hydrology, 6:68, 2019.
659 Grusson, Y., Antil, F., Sauvage, S., and Perz, S.: Testing the SWAT Model with Gridded
660 Weather Data of Different Spatial Resolution. Water, 9:54, 2017.
661 Guermazi, E., Milano, M., and Reynard, E.: Performance evaluation of satellite-based
662 rainfall products on hydrological modelling for a transboundary catchment in northwest
663 Africa, Theo. App. Clim. 138, 1695-1713, 2019.
664 Habib, E., Haile, A. T., Tian, T., and Joyce, R. J.: Evaluation of the High-Resolution
665 CMORPH Satellite Rainfall Product Using Dense Rain Gauge Observations and Radar-
666 Based Estimates, J. Hydrmeteo., 13 (6), 1784-1798, 2012.
667 Haile, A. T., Habib, E., Elsaadani, M., and Rientjes, T.: Intercomparison of satellite
668 rainfall products for representing rainfall diurnal cycle over the Nile basin, Int. J. Appl.
669 Earth Obs. 21, 230-240, 2013.
670 Hu, Q., Yang, D., Li, Z., Mishra, A.K., Wang, Y., and Yang, H.: Multi-scale evaluation of
671 six high-resolution satellite monthly rainfall estimates over a humid region in China
672 with dense rain gauges, Int. J. Remote Sens. 35, 1272-1294, 2014.
673 Huffman, G. J., Bolvin, D. T., Nelkin, E. J., Wolff, D. B., Adler, R. F., Gu, G., Hong, Y.,
674 Bowman, K. P., and Stocker, E. F.: The TRMM Multisatellite Precipitation

675 Analysis (TMPA): quasiglobal, multiyear, combined-sensor precipitation estimates at
676 fine scales, J. Hydrometeorol. 8, 38-55, 2007.
677 Huffman, G.J., Bolvin, D.T., Braithwaite, D., Hsu, K., Joyce, R.J., Kidd, C., Nelkin, E.J., and
678 Xie, P.: Algorithm Theoretical Basis Document (ATBD), 2015.
679 Huffman, G.J., Bolvin, D.T., Braithwaite, D., Hsu, K., Joyce, R., Xie, P., and Yoo, S.H.:
680 NASA global precipitation measurement (GPM) integrated multi-satellite retrievals
681 for GPM (IMERG). In Algorithm Theoretical Basis Document (ATBD); NASA/GSFC:
682 Greenbelt, MD, USA, 2014.
683 Jiang, S., Liu, S., Ren, L., Yong, B., Zhang, L., Wang, M., Lu, Y., and He, Y.: Hydrologic
684 Evaluation of Six High Resolution Satellite Precipitation Products in Capturing
685 Extreme Precipitation and Streamflow over a Medium-Sized Basin in China, Water,
686 10, 25, 2017.
687 Joyce, R. J., Janowiak, J. E., Arkin, P. A., and Xie, P.: CMORPH: a method that produces
688 global precipitation estimates from passive microwave and infrared data at high spatial
689 and temporal resolution, J. Hydrometeo. 5, 487-503, 2004.
690 Kabite, G., and Gessesse, G.: Hydro-geomorphological characterization of Dhidhessa
691 River Basin, Ethiopia, Int. Soil and Water Cons. Res. 6, 175-183, 2018.
692 Kabite, G., Muleta, M.K., and Gessesse, B.: Spatiotemporal land cover dynamics and
693 drivers for Dhidhessa River Basin (DRB), Ethiopia, Mod. Earth Sys. Environ. 6,
694 1089-1103, 2020.
695 Katsanos, D., Retalis, A., and Michaelides. S.: Validation of a high-resolution
696 precipitation database (CHIRPS) over Cyprus for a 30-year period, Atmos.
697 Res. 169, 459-464, 2016.
698 Kidd, C., and Huffman, G.: Global precipitation measurement. Meteorol. Appl. 18,334-
699 353, 2011.
700 Kidd, C., Bauer, P., Turk, J., Huffman, G.J., Joyce, R., Hsu, K.L., and Braithwaite, D.:
701 Intercomparison of high-resolution precipitation products over northwest Europe. J.
702 Hydrometeorol. 13, 67-83, 2012.
703 Kimani, M.W., Hoedjes, J.C.B., and Su, Z.: An assessment of satellite-derived rainfall
704 products relative to ground observations over East Africa, Remote Sens. 9(5), 430,
705 2017.
706 Lakew, H.B., Moges, S.A., and Asfaw, D.H.: Hydrological Evaluation of Satellite and
707 Reanalysis precipitation products in the Upper Blue Nile Basin: A case study of Gilgal
708 Abbay, Hydrology, 4, 39, 2017.

709 Lemann, T., Roth, V., Zeleke, G., Subhatu, A., Kassawmar, T., and Hurni, H.: Spatial and
710 Temporal Variability in Hydrological Responses of the Upper Blue Nile basin,
711 Ethiopia, Water, 11, 21, 2019.
712 Li, D., Christakos, G., Ding, X., and Wu, J.: Adequacy of TRMM satellite rainfall data in
713 driving the SWAT modeling of Tiaoxi catchment (Taihu lake basin, China), J. Hydr.
714 556, 1139-1152, 2018.
715 Maggioni, V., Meyers, P.C., and Robinson, M.D.: A Review of Merged High-Resolution
716 Satellite Precipitation Product Accuracy during the Tropical Rainfall Measuring
717 Mission (TRMM) Era, J. Hydrometeor. 17, 1101-1117, 2016.
718 Maidment, R., Emily, B., and Matt, Y.: TAMSAT Daily Rainfall Estimates (Version 3.0).
719 University of Reading. Dataset. doi.org/10.17864/1947.112, 2017.
720 Meng, J., Li, Z., Hao, J., Wang, S. Q.: Suitability of TRMM Satellite Rainfall in Driving
721 Distributed Hydrological Model in the Source Region of Yellow River. J. Hydrol.
722 509, 320-332, 2014.
723 Moriasi, D. N., Arnold, J. G., Van Liew, M. W., Bingner, R.L., Harmel, R.D., and Veith, T.L.:
724 Model evaluation guidelines for systematic quantification of accuracy in watershed
725 simulations. Trans. American Socie. Agr. Bio. Eng. 50(3), 885-900, 2007.
726 Nebuloni, R., D'Amico, M., Cazzaniga, G., De Michele, C., and Deidda, C.: Rainfall
727 estimate using Commercial Microwave Links (CML): first outcomes of the
728 MOPRAM project. EGU2020-1040, 19th EGU General Assembly, EGU2017,
729 proceedings from the conference held 23-28 April, 2017 in Vienna, Austria., p.18576.
730 https://doi.org/10.5194/egusphere-egu2020-1040, 2020.
731 Neitsch, S.L., Arnold, J.G., Kiniry, J.R., and Williams, J.R.: Soil & Water Assessment
732 Tool-Theoretical Documentation Version 2009. Texas Water Resour. Inst, 2009.
733 Nesbitt, S.W., Gochis, D.J., and Lang, T.J.: The diurnal cycle of clouds and precipitation
734 along the Sierra Madre Occidental observed during NAME-2004: Implications for
735 warm season precipitation estimation in complex terrain, J. Hydrometeoro. 9, 728-
736 743, 2008.
737 Nguyen, T.H., Masih, I., Mohamed, Y.A., and Van Der Zaag, P.: Validating rainfall-
738 runoff modelling using satellite-based and reanalysis precipitation products in the Sre
739 Pok catchment, the Mekong River basin, Geosciences, 8(5), 164-184, 2018.
740 Oromia Water Works Design and Supervision Enterprise (OWWDSE).: Dhidhessa Sub-
741 Basin Soil Survey Report. Dhidhessa-Dabus Integrated Land Use Planning Study
742 Project. Unpublished, 2014.

743 Roth, V., Lemann, T., Zeleke, G., Subhatu, A.T., Nigussie, T.K., and Hurni, H.: Effects of
744 climate change on water resources in the upper Blue Nile Basin of Ethiopia, Heliyon,
745 4(2018) e00771, 2018.
746 Sahlaoui, Z., and Mordane, S.: Radar Rainfall Estimation in Morocco: Quality
747 Control and Gauge Adjustment. Hydrology, 6 (2):41, 2019.
748 Smiatek, G., Keis, F., Chwala, C., Fersch, B., and Kunstmann, H.: Potential of
749 commercial microwave link network derived rainfallfor river runoff simulations.
750 Environmental Research Letter, 12, 034026, 2017.
751 Seyyedi, H., Angagnostou, E.N., Beinghley, E., and McCollum, J.: Hydrologic evaluation
752 of satellite and reanalysis precipitation datasets over a mid-latitude basin, Atm.
753 Res. 164-165, 37-48, 2015.
754 Sirisena, T.A.J.G., Maskey, S., Ranasinghe, R., and Babel, M.S.: Effects of different
755 precipitation inputs on streamflow simulation in the Irrawaddy River Basin, Myanmar.
756 J. Hyd.: Reg. Studies. 19,265-278, 2018.
757 Sorooshian, S., Hsu, K.-L., Gao, X., Gupta, H. V., Imam, B., and Braithwaite, D.: Evaluation
758 of PERSIANN system satellite-based estimates of tropical rainfall, B. Am. Meteorol.
759 Soc. 81, 2035-2046, 2000.
760 Stisen, S., and Sandholt, I.: Evaluation of remote-sensing-based rainfall products through
761 predictive capability in hydrological runoff modeling, Hydrol. Proce. 24, 879-
762 891, 2010.
763 Su, J., Lü, H., Wang, J., Sadeghi, A., and Zhu, Y.: Evaluating the Applicability of Four
764 Latest Satellite-Gauge Combined Precipitation Estimates for Extreme Precipitation
765 and Streamflow Predictions over the Upper Yellow River Basins in China. Remote
766 Sens. 9, 1176, 2017.
767 Tapiador, F.J., Turk, F.J., Petersen, W., Hou, A.Y., García-Ortega, E., Machado, L.A.T.,
768 Angelis, C.F., Salio, P., Kidd, C., Huffman, G.J., et al., Global precipitation
769 measurement: Methods, datasets and applications. Atmos. Res. 104-105, 70-97, 2012.
770 Thiemig, V., Rojas, R., Zambrano-Bigiarini, M., and Roo, A. D.: Hydrological evaluation
771 of satellite-based rainfall estimates over the Vota and Baro-Akobo Basin, J.
772 Hydrology. 499, 324-333, 2013.
773 Tong, K., Su, F., Yang, D., and Hao, Z.: Evaluation of satellite precipitation retrievals and
774 their potential utilities in hydrologic modeling over the Tibetan Plateau, J. Hydrol.
775 519, 423-437, 2014.

776 Toté, C., D. Patricio, H. Boogaard, R. Van der Wijngaart, E. Tarnavsky, and Funk, C.:
777 Evaluation of Satellite Rainfall Estimates for Drought and Flood Monitoring in
778 Mozambique, Remote Sens. 7 (2), 1758-1776, 2015.
779 Vernimmen, R.R., Hooijer, A., Aldrian, E., and Van Dijk, A.I.: Evaluation and bias
780 correction of satellite rainfall data for drought monitoring in Indonesia, Hydrol.
781 Earth Syst. Sci., 16, 133-146, 2012.
782 Villarini, G., Krajewski, W.F.: Review of the different sources of uncertainty in single
783 polarization radar-based estimates of rainfall. Surv. Geophys., 31, 107-129, 2010.
784 WMO: World Meteorological Organization Guide to Hydrological Practices: Data
785 Acquisition and Processing, Analysis, Forecasting and Other Applications. Geneva:
786 Switzerland, 1994.
787 Worqlul, A.W., Maathuis, B., Adem, A.A., Demissie, S.S., Langan, S., and Steenhuis, T.S.:
788 Comparison of rainfall estimations by TRMM3B42, MPEG and CFSR with
789 ground-observed data for the Lake Tana basin in Ethiopia, Hydrol. Earth Syst. Sci.
790 18, 4871-4881, 2014.
791 Wu, H., and Chen, B.: Evaluating uncertainty estimates in distributed hydrological
792 modeling for the Wenjing River watershed in China by GLUE, SUFI-2, and ParaSol
793 methods, Ecol. Eng. 76,110-121, 2015.
794 Xian, L., Wenqi, W., Daming, H., Yungang, L., and Xuan., J.: Hydrological Simulation
795 Using TRMM and CHIRPS Precipitation Estimates in the Lower Lancang-Mekong
796 River Basin. China Geog. Sci. 29(1), 13-25, 2019.
797 Xie, P., and Arkin, A.: An Inter-comparison of Gauge Observations and Satellite Estimates
798 of Monthly Precipitation, J. Appl. Meteoro. 34, 1143-1160, 1995.
799 Xue, X., Hong, Y., Limaye, A.S., Gourley, J.J., Huffman, G.J., Khan, S.I., and Chen, S.:
800 Statistical and Hydrological Evaluation of TRMM-Based Multi-Satellite Precipitation
801 Analysis over the Wangchu Basin of Bhutan: Are the Latest Satellite Precipitation
802 Products 3B42V7 Ready for Use in Ungauged Basins? J. Hydrol. 499, 91-99, 2013.
803 Yohannes, O.: Water Resources and Inter-Riparian Relations in the Nile Basin: The
804 Search for an integrative Discourse. 270, 2008.
805 Yong, B., Chen, B., Gourley, J.J., Ren, L., Hong, Y., Chen, X., Wang, W., Chen, S., and Gong,
806 L.: Inter-comparison of the Version-6 and Version-7 TMPA precipitation products
807 over high and low latitudes basins with independent gauge networks: is the
808 newer version better in both real-time and post-real-time analysis for water resources
809 and hydrologic ext, J. Hydrol. 508, 77-87, 2014.

Zeweldi, D.A., Gebremichael, M., and Downer, C.W.: On CMORPH rainfall for streamflow simulation in a small, Hortonian watershed. J. Hydrometeorol. 12, 456-466, 2011.

Zhang, C., Chen, X., Shao, H., Chen, S., Liu, T., Chen, C., Ding, Q., and Du, H.: Evaluation and Inter-comparison of High-Resolution Satellite Precipitation Eastimates-GPM, TRMM, and CMORPH in the Tianshan Mountain Area. Remote sens. 10, 1543, 2018.

Zhang, Z., Tian, J., Huang, Y., Chen, X., Chen, S., and Duan, Z.: Hydrologic Evaluation of TRMM and GPM IMERG Satellite-Based Precipitation in a Humid Basin of China. Remote Sens. 11, 431, 2019.

Zhao, Y., Xie, Q., Lu, Y., and Hu, B.: Hydrologic Evaluation of TRMM Multisatellite Precipitation Analysis for Nanliu River Basin in Humid Southwestern China. Scie. Reports, 7, 2470, 2017.

Zhou, J., Liu, Y., Guo, H., and He, D.: Combining the SWAT model with sequential uncertainty fitting algorithm for streamflow prediction and uncertainty analysis for the Lake Dianchi Basin, China. Hydrol. Process. 28, 521-533, 2014.

825 **Appendix**

826 Appendix Table 1. List of rain gauge stations used for SREs evaluation.

S. No	Stations	Latitude	Longitude	Elevation	Remark
1	Bedele	8.3	36.2	2011	Within the basin
2	Gatira	8.0	36.2	2358	Within the basin
3	Gimbi	9.2	35.8	1970	Within the basin
4	Nedjo	9.5	35.5	1800	Within the basin
5	Anger	9.3	36.3	1350	Within the basin
6	Gida Ayana	9.9	36.9	1850	Within the basin
7	Arjo	8.5	36.3	2565	Within the basin
8	Jimma*	7.8	36.4	1718	Within the basin
9	Nekemte*	9.1	36.5	2080	Within the basin
10	Shambu	9.6	37.1	2460	Near the basin
11	SibuSire	9.0	35.9	1826	Within the basin
12	Bure	8.2	35.1	1750	Near the basin
13	Sokoru	7.9	37.4	1928	Near the basin
14	Gore	8.1	35.5	2033	Near the basin

827 *systematically removed from using for calibration as they are already used for SREs calibration.